Phys Chem Minerals (2003) 30: 76–87
DOI 10.1007/s00269-002-0295-x

ORIGINAL PAPER

C. W. Yong · M. C. Warren · I. H. Hillier
D. J. Vaughan

Theoretical studies of cation adsorption on hydroxylated α-$A1_2O_3$ (corundum): electronic structure calculations

Received: 29 April 2002 / Accepted: 23 October 2002

Abstract The adsorption of alkali metal cations on a hydroxylated corundum surface was investigated using high-level electronic structure calculations, with both cluster Hartree–Fock and periodic density-functional theory approaches. The work concentrates on the structural aspects of binding sites with threefold oxygen coordination at the basal (0001) surface. It was found that adsorption at different sites can give rise to a wide range of adsorption energies, which strongly depends on the freedom of surface hydrogen atoms to adjust their positions. Alkali metal adions from Li^+ to Cs^+ were studied with the cluster method, periodic plane-wave pseudopotential calculations being carried out for K^+ adsorption to validate the cluster results. A site above an octahedral interstice was found to be the least preferred for cation adsorption, despite having the lowest repulsion from surface aluminium atoms. The strongest adsorption was found over an aluminium atom in the second layer, because the hydroxyl groups could reorient towards the neighbouring octahedral interstices, and hence significantly decrease repulsion with the cation. The adsorption energy and the first three interlayer spacings parallel to the basal surface change systematically with ionic size for each adsorption site. Many of these trends extend to adsorption of Ca^{2+}, Co^{2+} and Pb^{2+}, which were also investigated, although a redistribution of $3d$ electrons in Co^{2+} results in strong adsorption even at an unfavourable site. The results suggest that it may be possible not only to predict adsorption behaviour for a wide range of elements, but also to use experimental measurements of interplanar separations to gain information about contaminated surfaces.

C.W. Yong
Daresbury Laboratory, Daresbury,
Warrington, Cheshire,WA4 4AD, England

M.C. Warren (✉) · D.J. Vaughan
Department of Chemistry, University of Manchester,
Manchester M13 9PL, England
e-mail: m.c.warren@man.ac.uk

I.H. Hillier
Department of Earth Sciences and Williamson Research Centre
for Molecular Environmental Science, University of Manchester,
Manchester M13 9PL, England

Introduction

Mineral surfaces play an important role in controlling the chemical compositions of environmental systems. In particular, the release, migration and entrapment of ionic species at mineral/water interfaces can determine the chemical compositions of fluids in soils, aquifers and surface waters (Stumm 1987; Evans 1989; Vaughan and Pattrick 1995). For this reason, studies of the chemical processes at mineral/water interfaces are crucial not only for understanding the cycling of elements at the Earth's surface, but also for an assessment of the environmental impact of toxic contamination as a result of human activities.

There has been a great deal of experimental work involving studies of the interactions (particularly sorption and desorption) between materials in solution and mineral surfaces. Whereas macroscopic experimental measurements (Hohl and Stumm 1976; Benjamin and Leckie 1981; Sposito 1986) have yielded information on the overall sorption behaviour of a particular ion, techniques such as extended X-ray absorption fine structure (EXAFS), spectroscopy and X-ray absorption near-edge structure (XANES) spectroscopy have yielded information at an atomistic level such as adion–surface atom bond lengths and coordination numbers (Brown et al. 1988; Bassett and Brown 1990). The mechanism of sorption of a particular species can then be discussed using such measurements. Alternatively, computational methods such as molecular dynamics (MD) have been used to predict surface reactivities and structure of the adion–mineral complex as well as the sorption mechanisms (Baram and Parker 1996; de Leeuw et al. 1996; McCarthy et al. 1996). However, fundamental under-

standing of such interactions often requires chemical knowledge at a molecular level. In this respect, electronic structure calculations provide a powerful method to investigate the nature of bonding and electronic structure of surface species, information not easily obtained from experimental work.

Electronic structure methods have been successful in modelling a wide range of mineral surface systems (Gillan et al. 1996), including MgO (Neyman and Rosch 1993), TiO_2 (Bates et al. 1998), SiO_2 (Lopez et al. 1999; Civalleri et al. 1999) and corundum (Kubicki and Apitz 1998; Wittbrodt et al. 1998; Batyrev et al. 1999; Tepesch and Quong 2000). Nevertheless, many aspects of the reactivity of mineral surfaces are still poorly understood. For example, how do the charges and sizes of ions affect their interaction with mineral surfaces? How are preferential sorption sites related to mineral structures? What are the bonding requirements for sorptions to take place? Although work has been published on the characterization of mineral surface sites and the nature of surface complexation (such as Hiemstra et al. 1989a,b; Sverjensky and Sahai 1996; Bargar et al. 1997; Koretsky et al. 1998), including many experimental and theoretical studies on simple ionic substrates such as MgO (Ferrari and Pacchioni 1996; Yudanov et al. 1997; Snyder et al. 2000), there is a lack of systematic investigation of general behaviour of ion adsorption onto mineral surfaces using electronic structure calculations.

The emphasis in the present work is on the nature of the chemical interactions between species at the surface and the substrate atoms. One of the advantages of using electronic structure methods is that the chemical nature of the interactions can be isolated from factors such as solution pH, ionic strength, sorption density and temperature. We have chosen α-Al_2O_3 (corundum) as a model system because it has been studied extensively, and the surface structures are relatively well understood (Mackrodt et al. 1987; Causa et al. 1989; Kim and Hsu 1991; Manassidis et al. 1993; Schildbach and Hamza 1993; Manassidis and Gillan 1994; Batyrev et al. 1999; de Leeuw and Parker 1999). Its structure is closely related to hydrated aluminium oxides such as gibbsite ($Al(OH)_3$), diaspore (AlOOH) and the "colloidal" aluminium hydroxides .

Surface interactions usually take place in aqueous media, and so natural mineral oxide surfaces are usually hydroxylated. To reflect this within simulations of a tractable size, we have investigated the adsorption of bare cations on "dry" hydroxylated (0001) corundum surfaces. The alkali metals have been chosen as species to interact with the surface because the chemistry of these ions is generally well understood. These elements are also of practical interest (Na and K play important roles in biological processes; ^{137}Cs is an important toxic by-product of nuclear power generation). We have studied other metal cations to compare their chemical behaviour with the alkali metals. These include Ca^{2+}, an alkaline earth metal; Co^{2+}, a transition metal, and Pb^{2+}, a toxic heavy metal.

Choice of surface and simulation methodology

To give meaningful results but still present a tractable computational problem, computer simulations of sorption processes must employ a model system which not only represents the surface, the sorbate and the effects of hydration on both, but also minimizes the computational effort required to deal with non-essential effects. The most common simplifications are to study only the most stable surface and to ignore its detailed topography by constructing a single flat facet, and we adopt these strategies in this work. Furthermore, we omit the water molecules that would form the bulk liquid, although in some cases a single coordinated water molecule has been added outside the adion. However, it is well known that alumina and many other mineral surfaces will incorporate water molecules into the surface structure, and since this will have a major effect on sorption mechanisms, we include this effect in our model system. We now describe the construction of this model.

The Al_2O_3 crystal structure consists of an approximately hexagonal close-packed arrangement of O^{2-}, with two-thirds of the octahedral interstices occupied by Al^{3+}. Each O^{2-} is thus tetrahedrally coordinated by Al^{3+}. Parallel to the basal plane (0001), the structure has stacking sequences with two Al^{3+} ions sandwiched between two layers of O^{2-} (Fig. 1). The strong repulsion between the Al^{3+} ions causes distortion away from a common plane and results in two inequivalent Al–O distances of 1.86 and 1.97 Å (Wyckoff 1978).

The α-Al_2O_3 surface in vacuum is generally agreed to be Al-terminated, from fundamental considerations of dipoles at the surface, the predictions of a number of theoretical studies (Manassidis et al. 1993; Puchin et al. 1997; Batyrev et al. 1999) and recent experimental studies (Gautier et al. 1994; Ahn and Rabalais 1997; Guenard et al. 1998). These investigations also showed considerable relaxation at the surface, with the top O–Al interlayer spacing decreasing by as much as 70%. On the other hand, spectroscopic measurements on laboratory-grown Al_2O_3 films indicate the existence of oxygen-terminated basal-plane surfaces (Jaeger et al. 1991; Chen and Goodman 1994; Libuda et al. 1994) but

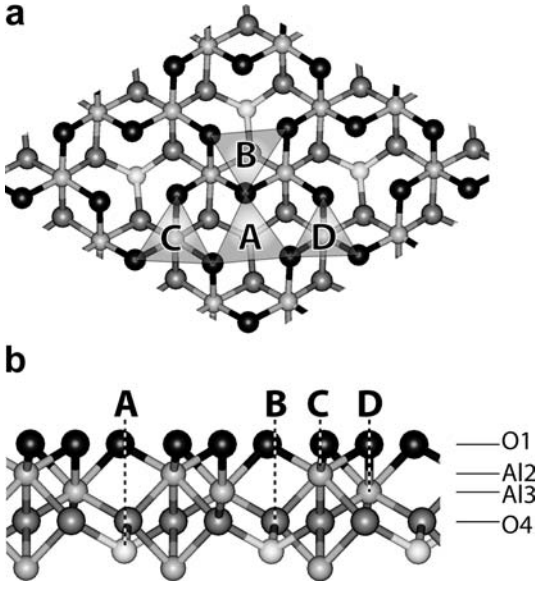

Fig. 1a,b **a** Top and **b** side views of the oxygen-terminated Al_2O_3 (0001) basal plane. Hydrogen atoms associated with surface hydroxylation have been omitted for clarity. *Shaded triangles* highlight the various threefold sites described in the text. The top (outer) layer of oxygens are *most darkly shaded*. The different layers of atoms parallel to the basal plane are designated with the labels as shown in **b**. The unit cell identified in **a** was used for the periodic calculations

variable stoichiometry affected those experiments so their results may not be applicable to pure corundum.

However, naturally occurring Al_2O_3 in solution will be hydrated. Considerable progress has been made in the past few years in determining the nature of the hydrated surface. Full hydroxylation was indicated by the results of high-resolution electron-energy-loss spectroscopy (HREELS) experiments (Coustet and Jupille 1994) which show that the surface -OH groups give rise to a single peak consistent with the existence of only one type of surface bridging oxygen on the (0001) basal plane. Theoretical calculations show that water readily dissociates to give surface hydroxyl groups on clean Al-terminated surfaces (Wittbrodt et al. 1998; Hass et al. 2000), and that the resulting hydroxide surface is stable with respect to the loss of water molecules (Nygren et al. 1997). Higher water coverage may break Al-surface bonds to give an oxygen-terminated surface (Hass et al. 2000), but even if a surface were terminated by oxygen atoms, one would assume that they were also stabilized by hydrogenation: recent theoretical calculations further demonstrated the stability of an —OH terminated surface (Di Felice and Northrup 1999).

To represent the hydrated surface in our model, therefore, we terminated a (0001) surface at a layer of oxygens, each of which was then hydroxylated. Compared to the stable surface in vacuum, this is equivalent to replacing each terminating Al by three H atoms. Indeed, representing the surface using a single layer of hydroxyl termination is an approach that has been used in previous MD simulations (Jin et al. 2000). The Al–O–H termination thus proposed is similar to the structure of layers within hydrated oxide minerals such as diaspore and gibbsite.

Figure 1 shows the top and side views of an oxygen-terminated Al_2O_3 (0001) surface. For clarity, only the topmost four layers of atoms are shown. The complexity of the surface means that there are several different threefold oxygen sites (active sites) at which a cation might be adsorbed. These sites are labelled: site A – on top of an octahedral interstitial oxygen; site B – on top of a tetrahedral interstitial oxygen; site C – on top of an underlying Al atom from the first layer of Al atoms; site D – on top of an underlying Al atom from the second layer of Al atoms. From simple geometric considerations, one might expect site A to be preferred, since the electrostatic repulsions between adions and Al atoms would be minimized; site C would then be the least preferred because the surface Al atom would be closest to the adion. Cation adsorption at these four sites is investigated in this work, using two computational methods described in the following section.

Computational methods

Most calculations were carried out for an isolated cluster taken from around the adsorption site and at the Hartree–Fock (HF) level, allowing a number of adion species to be studied. This requires only modest computational resources, but risks producing spurious effects from the finite extent of the cluster and the associated neglect of long-range electrostatic interactions. To assess the validity of the cluster approach, the adsorption of K^+ was studied in periodic simulations with density-functional theory (DFT): in this method, adions are adsorbed periodically onto an infinite slab with surfaces on both sides, so that a repeating supercell may be used and edge effects are avoided. However, there will then be interactions between adjacent adsorption sites, on both the surface and the next slab, and the periodic method is also much more computationally demanding. Both these geometries (cluster and periodic) have been used, with the same levels of theory, to study adsorption and dissociation of water (Hass et al. 2000), where it was shown that although very small clusters were inadequate, the energy of adsorption well away from cluster edges differed from values from periodic calculations by less than 15%. The combination of simulations with clusters of a reasonable size with a smaller number of periodic calculations for corroboration of results thus seems an appropriate way to proceed.

Cluster calculations with Hartree–Fock theory

Cluster calculations were carried out using the GAUSSIAN 98 programs (Frisch et al. 1998). The Al_2O_3 substrate was represented by clusters of atoms with appropriate hydrogen termination at the edges as well as at the surface as described above. In order to investigate all available sites, two independent cluster models were constructed as shown in Fig. 2. Cluster I provides a model for site A, whereas cluster II provides a model for sites B, C and D. These relatively large surface clusters are used in order to ensure that the active sites are completely surrounded by atoms. This is both to avoid unrealistic interactions between adions and terminal atoms, and to maintain the appropriate crystal structures at the active sites.

Adsorption was then simulated by placing an adion near each adsorption site in turn, and optimizing its position and those of nearby surface atoms. The stabilities of adsorption complexes could then be calculated by considering the reaction

$$\text{cluster} + \mathrm{M}^{n+} \rightarrow [\text{M-cluster}]^{n+}\ \text{complex}\ , \qquad (1)$$

where M^{n+} is the cation (adion) and the reaction energy is the adsorption energy, ΔE given as

$$\Delta E = E([\text{M-cluster}]^{n+}) - [E(\text{cluster}) + E(\mathrm{M}^{n+})]\ , \qquad (2)$$

where E is the energy with no zero point correction. A more negative value of ΔE thus indicates stronger adsorption.

In order to reduce computational costs, only the valence electrons have been considered, and only at the Hartree–Fock (HF) level. All ionic cores were treated by effective core potentials (Stevens et al. 1984). All cations were assigned effective core

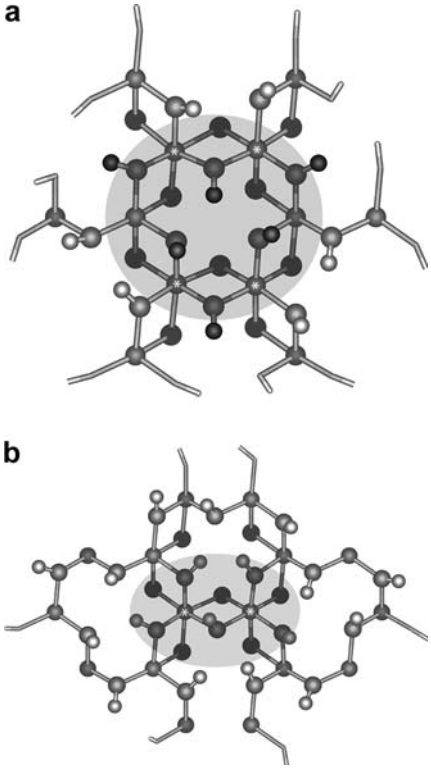

Fig. 2a,b Optimized structures of cluster models (**a** cluster I and **b** cluster II) showing different levels of calculation. Point charges are omitted for clarity. A1 atoms marked with *asterisk* are allowed to move during the optimization process. (1) *Shaded areas* have CEP-31G* on the surface oxygen, CEP-31G on Al atoms and bottom oxygen atoms and 6-31G on H atoms. (2) Atoms *drawn* as *spheres* are core Al atoms, oxygens with CEP-31G or H with 6-31G. (3) Outer regions *drawn only* as *sticks* consist of terminal hydroxyl groups with CEP-31G on oxygen atoms and STO-3G on hydrogen atoms

LanL2DZ basis sets (Hay and Wadt 1985) without further modification. The clusters were divided into several regions treated with different levels of basis set:

1. The active site, at the centre of the surface cluster where cation sorption would take place. Here, split-valence CEP-31G basis sets (Stevens et al. 1984, 1992; Cundari and Stevens 1993) on Al atoms and bottom oxygen atoms, CEP-31G* on surface bridging oxygen atoms, and 6-31G on H atoms, were used.

2. The intermediate region. The oxygen atoms were treated with CEP-31G basis sets, and the Al atoms treated as pseudoatoms with a formal charge fixed at +3. This means that only core *atoms* are present, which introduces Pauli repulsions and prevents other atoms from collapsing onto them. Such an approach not only reduces computation time but also acts as a buffer zone to separate the atoms at active sites from point charges (Stefanovich and Truong 1997). This also prevents the O^{2-} from being polarized towards the point charges, depleting the electron density at the surface (López and Illas 1998).

3. The outer region. The terminal O atoms were singly terminated with H atoms (initially with O–H parallel to the surface) and CEP-31G and minimal STO-3G basis sets were assigned to O and H atoms, respectively. These regions act as terminations of the surface cluster, where direct reactions between the sorbates and the atoms in these regions can be avoided.

To represent the effect of the bulk crystal, up to 75 point charges were introduced beneath the cluster, and the bottom was terminated with hydrogen point charges. Formal charges of +3, −2 and +1 were used for Al, O and H, respectively, since α-Al_2O_3 can be regarded as essentially ionic (Baxter et al. 2000). Point charges were not added in the surface plane, since H atoms tend to detach from terminal oxygen atoms and collapse towards adjacent strong negative point charges (oxygens) during optimization. Although less than 100 point charges were used rather than the several hundred normally used to reproduce the correct Madelung potential, our calculations show that the addition of extra point charges further beneath the surface does not significantly affect interplanar spacings and surface reactivities.

Only certain Al cations (marked * in Fig. 2) and all surface oxygen atoms in active sites as well as all H atoms have been allowed to move during the optimization steps. The rest of the atoms and all point charges are held fixed in order to preserve overall surface structures.

All energy values were compared at the Hartree–Fock (HF) level. This should be sufficient because we are interested mainly in the relative values of ΔE between different cations; absolute values are less important, so the highest levels of theory or basis sets were not justified. To verify the applicability of HF theory to this case, we carried out single point energy calculations on models with pseudocore basis sets using the B3LYP functional (Becke 1993), which is a hybrid of HF exchange and a DFT correlation density functional. We found that the differences in ΔE between the HF and B3LYP methods for alkali metal adions are in the order of 1–3 kcal mol^{-1}, or up to 5% of the HF value, indicating that we can safely use ΔE values calculated at the HF level. However, in the case of Co^{2+}, the difference is 35 kcal mol^{-1} (13% of the HF value), so electron correlation may be more important for transition metals.

To test the validity of the basis sets and the effective core potentials, we carried out a series of HF calculations of alkali metal ions adsorbed on a small neutral cluster $Al_2(OH)_6(H_2O)_4$, first using the pseudocore basis sets described above, and then with all electron calculations using 6-31G* basis sets on all substrate atoms and LanL2DZ on adions. We also examined adsorption of Co^{2+}, as a representative of the other adions discussed in this paper. The all-electron calculations and valence-electron-only calculations gave very similar optimized structures in all cases, with the variation in bond lengths between these approaches being typically less than 0.01 Å. We are therefore confident that the sets of basis functions used for our surface models can be used reliably for geometry optimizations.

Other possible errors from finite basis sets may arise from the so-called basis set superposition error (BSSE). We have used the counterpoise correction (Boys and Bernardi 1970) in order to estimate the extent of BSSE effects. The corrections usually give positive values, since superposition of two basis sets usually overestimates changes in energy. However, we have obtained negative values in most cases. The alkali metal–surface complexes give corrections of the order of 10 kcal mol^{-1}. The BSSE is negative because the surface cluster components of the surface–metal complexes are highly distorted, with considerably higher energies than the isolated surface clusters. In order to enable comparisons to be made among the various adions, similar basis sets have been used for all species: the BSSE is thus expected to be of a similar order of magnitude for each and has thus been neglected for these calculations, in common with previous studies (Kubicki et al. 1997).

Periodic calculations with density-functional theory

Our simulations were carried out with the CASTEP code (Payne et al. 1992; MSI 1998; Milman et al. 2000) and norm-conserving pseudopotentials that were found to be reliable for $MgAl_2O_4$ (Warren et al. 2000). The generalized gradient approximation (GGA) was used for electron exchange and correlation. The band structure was sampled with a $3 \times 3 \times 1$ Monkhorst–Pack k-point set, and a plane-wave basis set of up to 900 eV was used. Increasing this energy cutoff to 1000 eV decreased the total energy by 20 meV $atom^{-1}$. Following optimization of the primitive bulk unit cell, a hexagonal simulation cell with $a = b = 4.706$ Å, $c = 25.7$ Å and $\gamma = 120°$ was used, to accommodate one (0001) surface unit cell in the xy plane, containing a slab of eight O layers and seven double Al layers. Although this slab is repeated along z as well as parallel to the surface, over 9 Å of vacuum separates adjacent slabs, so negligible interaction between neutral slabs is expected. The unit cell was held fixed, to simulate the effect of bulk corundum below the surface.

Initially, an Al-terminated surface was simulated, with no hydrogens, to verify our simulations against previous periodic calculations of this surface (Hass et al. 1998; Batyrev et al. 1999; Wander et al. 2000). As expected, a large relaxation of the surface Al layer was found, until the Al atoms lay almost in the same plane as the first O layer. However, the absolute value of this contraction has been shown to vary significantly with the approximation used for exchange and correlation and other computational parameters (Batyrev et al. 1999; Wander et al. 2000) and is not easily tested experimentally.

The slab was then terminated in the same way as the cluster calculations, giving three hydroxylated oxygens in the (1×1) surface unit cell on each side of the slab and preserving neutrality. The OH groups were all initially oriented along [0001], perpendicular to the surface. The four adsorption sites (A–D) identified above are all present in this cell, as shown in Fig. 1.

Results and discussion

Surface cluster models

Table 1 shows the calculated interplanar spacings of the four outermost layers parallel to (0001) after optimiza-

Table 1 Comparison of interplanar spacings, in Å, for a bare hydroxylated surface in the cluster simulations

Spacings	Cluster I	Cluster II	Average	Nygren et al. (1997)	Bulk
OL1–AlL2	0.635	0.747	0.69	0.79	0.74
AlL2–AlL3	0.491	0.516	0.50	0.54	0.67
AlL3–OL4	0.894	0.734	0.81	0.82	0.74

tion. The labels used for atom layers are defined in Fig. 1b: OL1 represents the average for the surface oxygens; AlL2 and AlL3 represent the first and second layers of Al atoms, immediately below the surface oxygens; and OL4 refers to the first internal oxygen layer. These results show good agreement with those of Nygren et al. (1997), which were based on minimization calculations on periodic surfaces. Both sets of results show a slight reduction of AlL2–AlL3 spacings compared with the bulk values, whereas the AlL3–OL4 separation shows a slight increase. Our results predict a slight contraction of the OL1–AlL2 spacing by 0.05 Å from the bulk value. This is in contrast to those from simulations using empirical potentials (Nygren et al. 1997), which found an expansion by the same amount, compared with the bulk value. Nevertheless, our results show that hydroxylating the surface greatly reduces interplanar relaxation, as predicted previously (Nygren et al. 1997; Wittbrodt et al. 1998; Hass et al. 2000). Thus, our results show only a small (6.8%) decrease in distance between the OL1 plane and the AlL2 plane, which causes a corresponding reduction of Al–O distances to 1.77 and 1.92 Å from bulk values of 1.86 and 1.97 Å, respectively.

The positions of OH bonds after optimization of both clusters can be seen in Fig. 2. Some of the surface hydrogen atoms can be seen to lie nearly flat along the surface, lying over the top of the octahedral interstice. Most of these come within 2.3 Å of oxygen atoms on the other side of the interstice (shortest H...O distance is 2.09 Å, from a hydrogen atom in the active region) and so hydrogen bonding is very likely. Most of the hydrogen atoms that are not adjacent to the octahedral holes point away from the surface plane. Very similar surface arrangements have previously been deduced from DFT studies, firstly of dynamic simulations at 300 K (Hass et al. 2000) and secondly of a number of possible schemes for surface termination (Di Felice and Northrup 1999).

In order to test crystal plane relaxations on smaller systems, we also carried out all electron calculations at the HF level on isolated neutral clusters with no point charges. These clusters are slightly smaller in size but correspond to cluster I and cluster II. We used 6-31G basis sets on all atoms and found more extreme variations in the interplanar spacings. For example, the neutral cluster corresponding to cluster II gives OL1–AlL2, AlL2–AlL3 and AlL3–OL4 spacings with values of 0.65, 0.30 and 0.90 Å, respectively. This shows the importance of introducing point charges and of using larger systems in order to reproduce the surface structures properly.

Table 2 lists the average atomic charges for atoms on active sites for both optimized clusters. These values were determined by Mulliken analysis (Mulliken and Ermler 1977) and natural population analysis (NPA) (Glendenning et al. 1990). Charges determined by natural population analysis are generally larger than those determined using the Mulliken method, and so only like-with-like comparisons should be made. The charges on Al atoms determined by natural populations are comparable to the +1.9 derived from a bare Al-terminated surface (Wittbrodt et al. 1998). However, the surface oxygens have average charges of −1.29 ± 0.02 in both clusters. These values are slightly smaller than those calculated by Wittbrodt et al. of −1.66. This is not surprising, since the presence of H atoms would redistribute charges on the surface and reduce the electron densities of the surface O atoms. Based on the results shown in Tables 1 and 2, we conclude that the two surface clusters are chemically very similar, and that differences due to the choice of such model clusters are not significant.

Table 2 Differences between average atomic charges for atoms in the optimized cluster I and cluster II. Absolute values are sensitive to the methods and basis sets used

Populations	Atoms	Cluster I	Cluster II
Mulliken	Al	+1.47	+1.33
	O	−1.14	−1.14
	H	+0.57	+0.53
Natural	Al	+2.16	+2.13
	O	−1.29	−1.29
	H	+0.57	+0.54

Periodic calculations of surface

The hydrogen atoms were initially placed directly above the surface oxygen atoms, but all positions in the periodic slab were then fully optimized, giving the structure shown in Fig. 3. It can be seen that one of the three hydrogens per surface unit cell lies almost flat in the plane of the surface, pointing towards the top of the octahedral interstice (site A). This structure is qualitatively similar to that found in the cluster calculations, and the ratio of 1:3 matches that in other studies (Di Felice and Northrup 1999; Hass et al. 2000). Such an arrangement breaks the hexagonal symmetry still seen experimentally (Ahn and Rabalais 1997), but must be assumed to represent only a snapshot from a dynamic structure, rearrangements on a time scale of ~0.1 ps being observed in dynamic simulations (Hass et al. 2000).

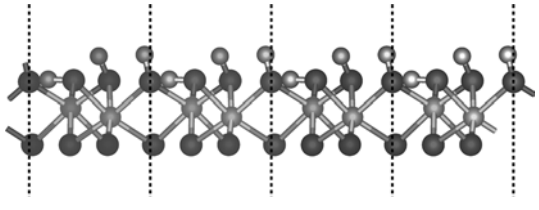

Fig. 3 Optimized structure of one side of the hydroxylated periodic slab, showing the hydrogen atoms and the first three layers of the Al_2O_3 surface (O, double Al layer, O). It can be seen that of the three hydrogen atoms per surface unit cell, one lies very nearly in the plane of the surface and the other two are nearly normal to the surface

The length of the "flat" OH bond is 0.98 Å compared to an average of 0.96 Å for those nearly vertical; these values match those reported by Hass et al. (2000) from snapshots of dynamical simulations. The H atoms in the "flat" OH groups are then only 2.08 Å on average from O atoms on the other side of site A, again indicating the likelihood of hydrogen bonding. Calculations of Mulliken charges gave these hydrogen atoms as 0.2|e| more positively charged than the others, and the O in this bond 0.1|e| more positive than its counterparts.

The electrostatic potential was calculated just above the hydroxylated surface, without any adsorbed ions. With the H ions in their equilibrium positions, there are only two metastable sites, both above oxygens below the surface, corresponding to position B. The variation in O–H orientation having broken the symmetry, one can identify a site B_1 adjacent to the hydrogen lying in the plane of the surface and B_2 opposite to that hydrogen. According to this analysis, B_2 is the more stable of the two, but this makes no allowance for further reorientation of the O–H bonds in response to adsorption.

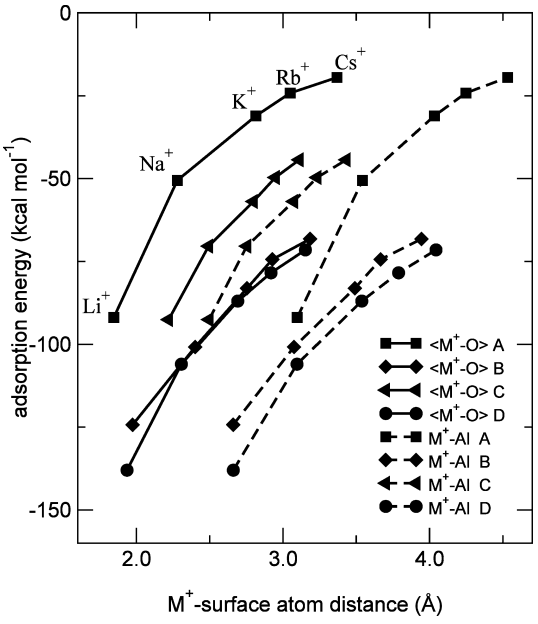

Fig. 4 Variation of adsorption energy and distance to closest atoms in the surface for alkali metals at different sites

Adsorptions of cations

In both cluster and periodic calculations, an adion was initially placed on top of a threefold site and both it and ions in the surface were allowed to relax. For sites which were not the most favoured, adions eventually tended to move away towards the most stable site, indicating that other sites did not even provide local maxima in the adsorption energy. While this confirmed the identification of the most stable site, it prevented immediate calculation of the adsorption energy differences between sites. Slightly different strategies were used in the two simulation methods to obtain estimates of the relative adsorption energies of the sites. In the cluster calculations, the adion was returned to its last position before starting significant lateral movement, to obtain an appropriate height, and then fixed while the optimization continued with only the surface atoms allowed to move; fine adjustment of the adion's fixed position was also carried out as an iterative process. In the periodic simulations, the K^+ ion was fixed at the exact crystallographic position in the plane of the surface (the *ab* plane), and its height above the surface (parallel to *c*) allowed to vary during full optimization of the ions in the slab.

Figure 4 shows the calculated values of adsorption energies, ΔE, (also given in Table 3) and average distances to the nearest surface atoms, from the cluster calculations with alkali metal ions on each of the four sites in turn. The clusters used were described above and are shown in Fig. 5. The results show large variations in ΔE over the different sites but, as might be expected, systematic trends are found at each site. Moving from Li^+ to Cs^+ above each site, the strength of adsorption decreases and average M^+–O and nearest M^+–Al distances increase. According to the NPA calculations

Table 3 Values of adsorption energies, ΔE (kcal mol^{-1}) for alkali metal ions adsorbed on various threefold sites. See text for the definitions of the sites

Metal ions	Site A	Site B	Site C	Site D
Li^+	−91.89	−124.3	−92.56	−138.0
Na+	−50.35	−100.8	−70.38	−106.0
K^+	−31.06	−83.09	−56.90	−86.96
Rb^+	−24.16	−74.37	−49.65	−78.42
Cs^+	−19.48	−68.21	−44.33	−71.51

(described further below), the main change upon adsorption of the metal cation is in the occupation of electrons in the outer *s* orbital, indicating that the attraction is not purely ionic.

To date, we are not aware of previous work on the alkali metals with which our ΔE values can be compared. DFT simulations of adhesion of Cu adatom binding on this surface (Niu et al. 2000) gave adhesion values of between 0.3 eV (7 kcal mol^{-1}) and 5.2 eV per atom (120 kcal mol^{-1}), depending on the adsorption site and Cu coverage. Calculations of the binding energy of Rb^+ on the clean (001) surface of MgO (Ferrari and Pacchioni 1996) give only about 5 kcal mol^{-1} compared with the smallest value of about 24 kcal mol^{-1} obtained in this work. Compared to MgO, our larger values arise because the adion can bind to three oxygens, even though the Al_2O_3 surface is hydroxylated, whereas on the MgO surface adsorption occurs directly above a single surface oxygen. We have performed calculations involving placing the adions directly on top of a surface oxygen in our model. In all cases, the adions move towards one of the threefold sites (in most cases, towards site D) during optimizations. Furthermore, the repulsion

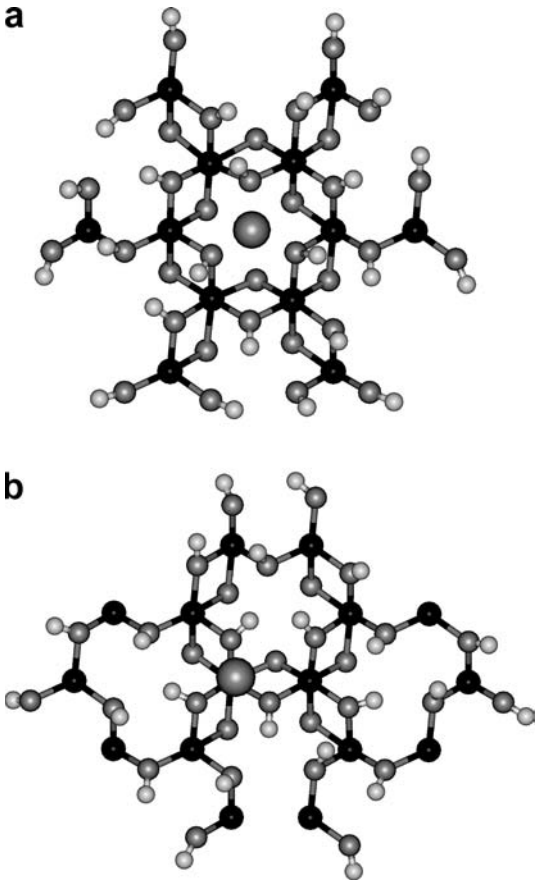

Fig. 5a,b Optimized structures for adsorption of **a** Na^+ at site A, and **b** Na^+ at site D. Only atoms involved in quantum mechanical calculations are shown

between adions and surface cations would be expected to be much stronger on the (001) surface of MgO compared with Al_2O_3(0001), since the Mg^{2+} is present at the surface, whereas the Al^{3+} is shielded by the top layer of oxygens. It is therefore not surprising that we have found hydroxylated Al_2O_3 to give stronger adsorption than MgO.

It is interesting that site D is predicted to give the strongest binding energy, even though the adions are directly above an Al cation, and it is site A that gives the weakest adsorption despite having the largest M^+–Al distance. We believe this counterintuitive behaviour to be due to differences in the steric arrangement of surface H atoms. Before adsorption, about two-thirds of the O–H bonds point out of the surface. However, when a positive adion approaches, their orientation may change in order to minimize the repulsion with the adion. The final value of ΔE will therefore depend on how these H atoms are arranged. The importance of O–H orientation was also found in studies of Cu adsorption (Niu et al. 2000).

This important role of OH orientation is illustrated in Fig. 5, which shows the optimized structures for Na^+ adsorption at sites A and D. With adsorption at site D, the OH bonds on the three nearest oxygen atoms are all predicted to lie flat along the surface plane, pointing towards the neighbouring octahedral interstice. Not only does this minimize the H–Na^+ repulsion, but it also enables hydrogen bonding to other oxygens, across the octahedral site. However, for adsorption at A, the much smaller neighbouring tetrahedral interstices do not favour the accommodation of H atoms, which would have to be in closer proximity to Al atoms. As a result, the nearest OH bonds lie out of the surface plane, increasing repulsion of H with the adion. This is, however, partially counteracted by attraction between the surface oxygens and the adion.

For all alkali metal adions, values of ΔE from the cluster calculations follow the trend of site D > site B > site C > site A, but with B only very slightly less stable than D. In the following sections we will attempt to understand the reasons for this ordering.

Periodic calculations with K^+

In the periodic DFT calculations with K^+, the orientations of OH bonds were also found to respond significantly to adsorption. However, in contrast to the cluster results, site B was found to be the most stable. When K^+ was placed on all other sites, it migrated to another tetrahedrally coordinated B site. Each (1×1) surface unit cell contains one K^+, three H atoms and one octahedral interstice, so orientation of all three OHs into this space would bring them into very close proximity. The energy-lowering mechanism demonstrated in the cluster calculations is therefore disabled in periodic calculations with a 1×1 unit cell: larger unit cells would be needed to reproduce the effect. Our periodic calculations gave site A as the next most favourable, in line with the initial expectations based on M^+–Al distances.

Competing effects in adsorption

Having identified that the positions of the H atoms are very important, we now consider in more detail the factors determining adsorption energy. From the NPA results, we conclude that the binding is primarily ionic. If so, it is reasonable to assume that the value of ΔE is a balance between attractive (A) and repulsive (R) interactions:

$$\Delta E = -A(\mathrm{M^+\!\!-\!\!O}) + R(\mathrm{M^+\!\!-\!\!H}) + R(\mathrm{M^+\!\!-\!\!Al}) + R(\mathrm{internal}) \ . \quad (3)$$

The first three terms represent interactions between the adion and atoms in the surface, and can be considered as a net attraction, denoted A(external). The attractive forces largely arise from attraction between the adions and the surface oxygens. These are partially countered by electrostatic repulsions between adions and hydrogen atoms, R(M^+–H), and between adions and surface cations, R(M^+–Al).

The last term in Eq. (3), R(internal), arises from the energy cost of changes in surface structure in response to the adion. This term includes H–H repulsion and the energy of compression or expansion of layers. The value of R(internal) can be estimated from the energy difference between the optimized bare surfaces and an adion–surface complex with the adion removed but the structure maintained, its values for different adions and sites being shown in Fig. 6. Note that with the exception of Li^+, there are only small differences in repulsive energies between sites B, C and D, for all of which there are three adjacent octahedral interstices. Li^+ may show anomalous behaviour because of its charge/size ratio. It can be seen that, like ΔE, the magnitude of this energy decreases from Li^+ to Cs^+: as the M^+–O distance increases (Fig. 5) the M^+–H repulsion should decrease, giving a weaker driving force for OH reorientation and other changes in the surface.

By subtracting R(internal) from ΔE in Eq. (3), we obtain A(external), the energy from interactions between the adion and the distorted surface. The "external" energy itself depends on the reconfiguration of the surface structure, being not truly independent of R(internal). However, it can be seen (Fig. 6) that A(external) varies more widely than R(internal), across both species and sites For a given adion, if we assume that the strong attraction $A(M^+–O)$ is similar for all threefold sites, the variation in A(external) between sites depends mainly on the M^+–H and M^+–Al repulsions.

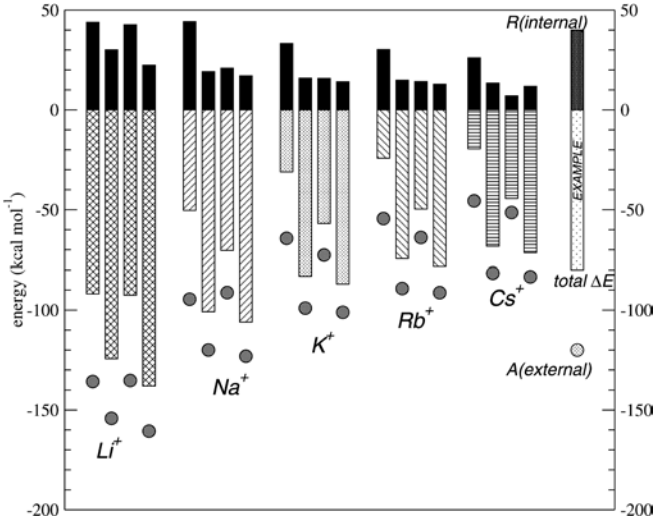

Fig. 6 Competition of internal (surface relaxation) and external (electrostatic attraction between adion and surface) energies to total adsorption energy. The *example bar on the right* illustrates the different contributions: (1) the *dark portion* with positive ΔE gives the internal energy cost of changing the Al_2O_3 surface structure in the absence of the adion; (2) the *shaded circle* at negative ΔE gives the decrease in energy due to external electrostatic attraction between adion and surface (external energy); (3) the *light portion of each bar*, with negative ΔE, gives the net ΔE of sorption (equal to the sum of internal and external energies); (4) the *combined height of each bar* is thus also equal to the external energy

We therefore deduce that sites A and C have repulsive effects similar to and much larger than sites B and D. The large repulsive effect at site C is largely due to repulsion between the adion and the first underlying layer of Al^{3+} ions. In contrast, adions at site A are generally farthest away from these aluminium cations, and so the large repulsive effects are believed to be mainly attributable to the $R(M^+–H)$. As a result of these repulsive effects, both sites A and C give the weakest adsorption. Sites B and D offer much less repulsion to adions, although A(external) is a slightly stronger for site D, probably because of the slightly larger value of $R(M^+–Al)$ there. Coupled with a slightly larger R(internal) at D, this leads to D having the strongest adsorption, albeit by a small margin.

Interplanar spacings of atom layers parallel to the basal plane

The capacity for large relaxations in the Al_2O_3 surface is illustrated in the extreme by the bare Al-terminated surface. Since these changes have been measured with X-ray scattering techniques (Guenard et al. 1998), we wish to investigate whether similar effects could be used to help deduce adsorption modes experimentally. Figure 7 shows the calculated change in interplanar spacings between the two outermost planes parallel to the surface, in the presence of adions at the different sites.

In general, there is an increase in the O1–Al2 layer separation due to attraction between the surface oxygen layer and the adions. The Al2–Al3 distance also increase in most cases, and aluminium layers are then pushed

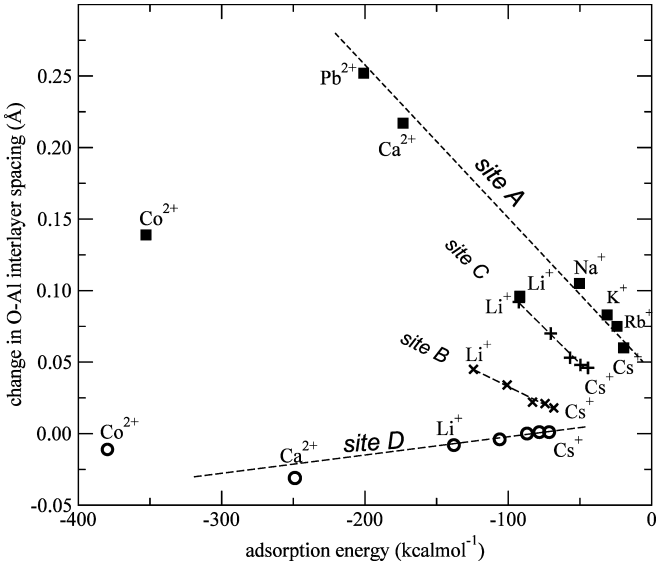

Fig. 7 Changes in the spacing between the first two layers of the surface, O–Al, for all adion species at various sites. The results for the alkali metals from Li^+ to Cs^+ follow the same order for each site, so only the end points are labelled for sites B (+ symbols) and C (x symbols)

away from the surface causing a decrease in Al3–O4 layer separation. It is interesting that these last two changes compensate for each other, such that the Al2–O4 separation is almost independent of adsorption site. This was also observed in the periodic DFT calculations for K^+, in which all atoms in the simulation relax, so it is not an artefact of the constraints on optimization in the cluster. For this reason, we have concentrated on the spacing between the outermost planes.

The changes in interplanar spacings reflect the trends already found for adsorption behaviour. They generally decrease in size from Li^+ to Cs^+, mirroring the decrease in adsorption energy. Generally, the smaller changes in layer spacings are found for sites B and D, which give the strongest adsorption. Conversely, the weak adsorption at site A is associated with a large change. The exceptionally large change caused by sorption of Li^+ on site C is because one of the oxygens loses its bond with an Al below it, and then moves much closer to the small Li^+ ion.

The periodic calculations, in which relaxation of H atoms are inhibited, did not give the very small change in the O1–Al2 spacing at D. Instead, site B gave the smallest adjustment, again coinciding with the strongest adsorption. The changes in interlayer spacings are therefore at least partly due to structural rearrangements at the surface, rather than solely due to the presence of the adion.

Adsorption of Ca^{2+}, Co^{2+} and Pb^{2+}

In order to widen our investigation of cation adsorption on (0001) Al_2O_3, we repeated the cluster calculations using Ca^{2+}, Co^{2+} and Pb^{2+} as representative divalent adions at sites A and D. We found that a bare Pb^{2+} ion at site D resulted in diffusion of the aluminium ion directly below (into the vacant octahedral interstitial site further beneath the surface), presumably because of strong electrostatic repulsion between the Pb^{2+} ion and the Al ion. This Al migration was also observed for other bare divalent cations such as Zn^{2+} and Cd^{2+} and numerical results from simulations in which migration occurred are not compared directly with results for simple adsorption. It is not clear whether the diffusion is a consequence of the nature of the adion or an artefact of the model. However, in fully hydrated systems some screening would arise from hydration clusters, since the dipole of a water molecule can partially counteract the repulsion from the charge of the bare cation. Simulations of partly hydrated adions are underway and will help to resolve this issue.

The results of simulations of simple adsorption are included in the comparisons of ΔE and the change in the outer (0001) interlayer spacing shown in Fig. 7. Due to the greater formal charge, the divalent cations are adsorbed much more strongly than the alkali metals. The net changes in interlayer spacing are again much greater for site A than for site D, and some of the trends relating ΔE and interlayer spacing for the alkali metals are continued. The steric effects discussed above suggest that ΔE should be related to both the charge and ionic radius of the adion. Ionic radii for octahedral coordination were used for all ions except Li^+, for which tetrahedral coordination was assumed, and Rb^+ and Cs^+, for which eightfold coordination was assumed; values were taken from Cotton et al. 1999. The ratios of charge to ionic radius for all the bare cations at site D (with the exception of Pb) are shown in Fig. 8 and display a trend for ΔE which encompasses very different types of cations. A larger range of cations would need to be investigated for this behaviour to be confirmed, but these results are encouraging in view of our desire to elucidate general trends. The adsorption on OH surface groups of Co^{2+} was found to be stronger than Pb^{2+} from EXAFS studies (Bargar et al. 1997).

Characterization of adsorption complexes

The nature of adsorption complexes was investigated using natural-bond orbital (NBO) calculations and natural population analysis (NPA) (Glendinning et al. 1990). The NPA atomic charges are directly related to the electron population, and are often used to characterize the nature of complex bonding and electron distribution by analyzing the population of natural electronic orbitals. Charges were calculated for the alkali metals at sorption sites A and D and showed only small (<0.1) electron populations in the valence *s* orbitals. Li^+ was the least positive ion ($+0.937$ at site A). The *s* population decreases on moving down the group (giving a charge of $+0.995$ for Cs at either site), indicating yet smaller covalent character. We therefore conclude that, in general, the bonds to the adion are predominantly ionic.

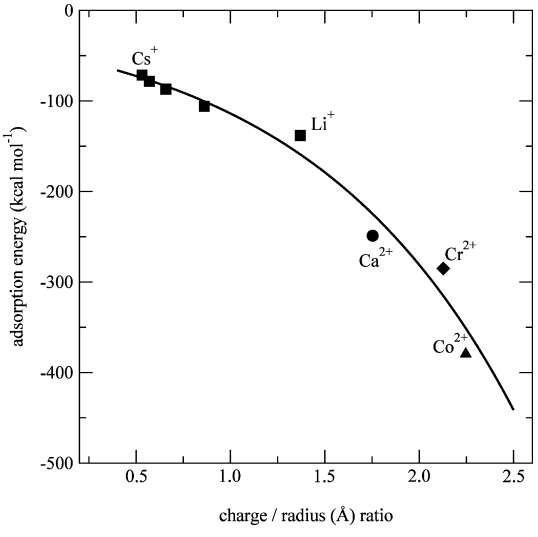

Fig. 8 Adsorption energy and charge/radius ratio for all adsorbed species at site D. The *line* is a guide to the eye

Since there are only very small differences between NPA charges on adions between sites A and D, we turn to atoms in the surface for differences in adsorption chemistry. The charges on O and H were averaged over the three OH surface groups surrounding sites A and D. When a cation approaches the surface, its electrostatic attraction might be expected to increase the electron population (decrease charge) at the surface.

At site A, Li^+ induces greater negative charge (−0.044e) on surface oxygens, following initial expectations, and a small increase in charge (0.015e) on hydrogen atoms. However, this effect is steadily reversed as cations become larger: from K^+ to Cs^+ the electron population on surface oxygens decreases (at site A, Cs^+ is 0.018e more positive) and the hydrogen atoms become less positive (−0.033e in the presence of Cs^+). With increasing ionic size, it becomes more difficult for the adions to interact with the surface oxygens without strong repulsion from the hydrogen atoms. This results in transfer of electrons to the hydrogen atoms in order to reduce the electrostatic repulsion exerted between them and the adion. This inherent compromise may also explain why site A has the smallest value of ΔE for all adion species.

In contrast, site D consistently shows surface oxygen atoms having gained electrons in the presence of an adion (charge changes by −0.046e for Li^+), and hydrogen atoms undergoing a slight loss of electrons (0.016e more positive charge for Li^+). This can occur at this site because the hydrogen atoms move towards the neighbouring octahedral interstices, and thus minimize their repulsion with adions. The effect weakens from Li^+ to Cs^+ (oxygen changes by −0.016e for Cs^+), and for hydrogen atoms in the presence of Cs^+ there may even be a small loss of electron population. Nevertheless, this charge-transfer mechanism may contribute to the strong adsorption found at site D.

Conclusions

Our electronic structure calculations on the adsorption of cations on the hydroxylated basal surface of α-$A1_2O_3$ have shown that adsorption at different sites can give rise to a wide range of adsorption energies even though, chemically, there is only one type of surface oxygen. We have shown for the anions studied that, with the exception of Li^+, the atomic charges are very similar for all sites, and that the interactions with the adions are predominantly ionic in character. The main reason for the differences in adsorption energies is thus the geometrical arrangement of surface atoms near to the active sites and not the actual chemistry of the surface. A very important factor is the freedom of surface hydrogen atoms to adjust their positions: this was demonstrated both in cluster calculations and indirectly as a result of perodic constraints. It is likely that this mechanism will give rise to changes in adsorption with increasing coverage, which should be detectable if future simulations with larger unit cells are performed.

A key objective of the kind of work presented here is to develop predictive rules governing the process of adsorption of metal ions on oxide mineral surfaces. The systematic changes observed in interlayer spacings parallel to the basal surface are therefore encouraging, since such changes should be experimentally accessible. The suggested relationship between charge/radius ratio and ΔE for bare ions indicates that a detailed knowledge of electronic configuration may not be necessary to estimate adsorption energies. Further developments of the approach presented here include modelling the effects of the presence of water molecules, and of a solvent "continuum", on sorption and will be reported in future publications.

Acknowledgements The authors thank the Natural Environment Research Council for support in carrying out this work.

References

Ahn J, Rabalais JW (1997) Composition and structure of the $Al_2O_3\{0001\}$-(1×1) surface. Surf Sci 388: 121–131

Baram PS, Parker SC (1996) Atomistic simulation of hydroxide ions in inorganic solids. Phil Mag (B) 73: 49–58

Bargar JR, Towle SN, Brown GE, Jr, Parks GA (1997) XAFS and bond-valence determination of the structures and compositions of surface functional groups and Pb(II) and Co(II) sorption products on single-crystal α-Al_2O_3. J Colloid Interface Sci 185: 473–492

Bassett WA, Brown GE, Jr (1990) Synchrotron radiation – applications in the Earth sciences. Annu Rev Earth Planet Sci 18: 387–447

Bates SP, Kresse G, Gillan MJ (1998) The adsorption and dissociation of ROH molecules on TiO_2 (110). Surf Sci 409: 336–349

Batryev I, Alavi A, Finnis MW (1999) Ab initio calculations on the Al_2O_3(0001) surface. Faraday Discuss 114: 33–43

Baxter R, Reinhardt P, López N, Illas F (2000) The extent of relaxation of the α-Al_2O_3 (0001) surface and the reliability of empirical potentials. Surf Sci 445: 448–460

Becke AD (1993) Density-functional thermochemistry, 3. The role of exact exchange. J Chem Phys 98: 5648–5652

Benjamin MM, Leckie JO (1981) Multiple-site adsorption of Cd, Cu, Zn, and Pb on amorphous iron oxyhydroxide. J Colloid Interf Sci 79: 209–221

Boys SF, Bernardi F (1970) The calculations of small molecular interaction by the difference of separate total energies. Some procedures with reduced error. Mol Phys 19: 553–556

Brown GE, Jr, Calas G, Waychunas GA, Petiau J (1988) In: Hawthorne FC (ed.), Spectroscopic methods in mineralogy and geology, Reviews in mineralogy, vol 18. Mineralogical Society of America, Washington DC, pp 431–512

Causa M, Dovesi R, Pisani C, Roetti C (1989) Ab initio characterization of the (0001) and (1010) crystal faces of α-alumina. Surf Sci 215: 259–271

Chen PJ, Goodman DW (1994) Epitaxial growth of ultrathin Al_2O_3 films on Ta(110). Surf Sci 312: L767–L773

Civalleri B, Casassa S, Garrone E, Pisani C, Ugliengo P (1999) Quantum mechanical ab initio characterization of a simple periodic model of the silica surface. J Phys Chem (B) 103: 2165–2171

Cotton FA, Wilkinson G, Murillo CA, Bochmann M (1999) Advanced inorganic chemistry. Wiley Interscience, New York

Coustet V, Jupille J (1994) High-resolution electron-energy-loss spectroscopy of isolated hydroxyl-groups on α-Al_2O_3(0001) Surf Sci 309: 1161–1165

Cundari TR, Stevens WJ (1993) Effective core potential methods for the lanthanides. J Chem Phys 98: 5555–5565

de Leeuw NH, Parker SC (1999) Effect of chemisorption and physisorption of water on the surface structure and stability of α-alumina. J Am Ceram Soc 82: 3209–3216

de Leeuw NH, Watson GW, Parker SC (1996) Atomistic simulation of adsorption of water on three-, four- and five-coordinated surface sites of magnesium oxide. J Chem Soc Faraday Trans 92: 2081–2091

Di Felice R, Northrup JE (1999) Determination of the α-Al_2O_3 (0001) surface relaxation and termination by measurements of crystal truncation rods. Phys Rev (B) 60: R16287–R16290

Evans LJ (1989) Chemistry of metal retention by soils – several processes are explained. Environ Sci Tech 23: 1046–1056

Ferrari AM, Pacchioni G (1996) Metal deposition on oxide surfaces: a quantum-chemical study of the interaction of Rb, Pd, and Ag atoms with the surface vacancies of MgO. J Phys Chem 100: 9032–9037

Frisch MJ, Trucks GW, Schlegel HB, Scuseria GE et al. (1998) Gaussian 98, Revision A-5, Gaussian Inc, Pittsburgh PA

Gautier M, Renaud G, Van LP, Villette B, Pollak M, Thromat N, Jollet F, Duraud J-P (1994) α-Al_2O_3-(0001) surfaces – atomic and electronic structure. J Am Ceram Soc 77: 323–334

Gillan MJ, Kantorovich LN, Lindan PJD (1996) Modelling of oxide surfaces. Curr Opin Solid State Mat Sci 1: 820–826

Glendenning ED, Reed AE, Carpenter JE, Weinhold F (1990) NBO, version 3.1; University of wisconsin: Madison, Wisconsin

Guenard P, Renaud G, Barbier A, Gautier-Soyer M (1998) Determination of the α-Al_2O_3(0001) surface relaxation and termination by measurements of crystal truncation rods. Surf Rev Lett 5: 321–324

Hass KC, Schneider WF, Curioni A, Andreoni W (1998) The chemistry of water on alumina surface: reaction dynamics from first principles. Science 282: 265–268

Hass KC, Schneider WF, Curioni A, Andreoni W (2000) First-principles molecular dynamics simulations of H_2O on α-Al_2O_3 (0001). J Phys Chem (B) 104: 5527–5540

Hay PJ, Wadt WR (1985) Abinitio effective core potentials for molecular calculations. J Chem Phys 82: 270–283 (Sc-Hg), 284–298 (Na-Bi), 299–310 (K-Au)

Hiemstra T, Van Riemsdijk WH, Bolt GH (1989a) Multisite proton adsorption modeling at the solid-solution interface of (hydr) oxides – a new approach, 1. Model description and evaluation of intrinsic reaction constants. J Colloid Interface Sci 133: 91–104

Hiemstra T, de Wit JCM, Van Riemsdijk WH (1989b) Multisite proton adsorption modeling at the solid-solution interface of (hydr)oxides – a new approach 2. Application to various important (hydr)oxides. J Colloid Interface Sci 133: 105–117

Hohl H, Stumm W (1976) Interaction of Pb^{2+} with hydrous γ-Al_2O_3 J. Colloid Interface Sci 55: 281–288

Jaeger RM, Kuhlenbeck H, Freund H-J, Wuttig M, Hoffmann W, Ibach H (1991) Formation of a well-ordered aluminum-oxide overlayer by oxidation of NiAl(110). Surf Sci 259: 235–252

Jin RY, Song K, Hase WL (2000) Molecular dynamics simulations of the structures of alkane/hydroxylated α-Al_2O_3(0001) Interfaces. J Phys Chem (B) 104: 2692–2701

Kim Y, Hsu T (1991) A reflection electron-microscopic (REM) study of α-Al_2O_3 (0001) surfaces. Surf Sci 258: 131–146

Koretsky CM, Sverjensky DA, Sahai N (1998) A model of surface site types on oxide and silicate minerals based on crystal chemistry: implications for site types and densities, multi-site adsorption, surface infrared spectroscopy, and dissolution kinetics. Amer J Sci 298: 349–438

Kubicki JD, Apitz SE (1998) Molecular cluster models of aluminium oxide and aluminium hydroxide surfaces. Am Mineral 83: 1054–1066

Kubicki JD, Blake GA, Apitz SE (1997) Molecular orbital calculations for modelling acetate-aluminatesilicate adsorption and dissolution reactions. Geochim Cosmochim Acta 61: 1031–1046

Libuda J, Winkelmann F, Bäumer M, Fruend H-J, Bertrams T, Neddermayer H, Müller K (1994) Structure and defects of an ordered alumina film on NiAl(110). Surf Sci 318: 61–73

López N, Illas F (1998) Ab initio modeling of the metal-support interface: the interaction of Ni, Pd, and Pt on MgO(100). J Phys Chem (B) 102:, 1430–1436

Lopez N, Illas F, Pacchioni G (1999) Ab initio theory of metal deposition on SiO_2.1.Cu_n ($n = 1$–5) clusters on nonbridging oxygen defects. J Phys Chem (B) 103: 1712–1718

Mackrodt WC, Davey RJ, Black SN (1987) The morphology of α-Al_2O_3 and α-Fe_2O_3 – the importance of surface relaxation. J Cryst Growth 80: 441–446

Manassidis I, Gillan MJ (1994) Structure and energetics of alumina surfaces calculated from first principles. J Am Ceram Soc 77: 335–338

Manassidis I, De Vita A, Gillan MJ (1993) Structure of the (0001) surface of α-Al_2O_3 from 1st principles calculations. Surf Sci Lett 285: L517-L521

McCarthy MI, Schenter GK, Scamehorn CA, Nicholas JB (1996) Structure and dynamics of the water/MgO interface. J Phys Chem 100: 16989–16995

Milman V, Winkler B, White JA, Pickard CJ, Payne MC, Akhmatskaya EV, Nobes RH (2000) Electronic structure, properties, and phase stability of inorganic crystals: A pseudopotential plane-wave study. Int. J Quant Chem 77: 895–910

MSI (1998) CASTEP user guide. Molecular Simulations Inc., San Diego

Mulliken RS, Ermler WC (1977) Diatomic molecules: results of ab initio calculations. Academic Press, New York p33

Neyman KM, Rosch N (1993) Bonding and vibrations of Co molecules adsorbed at transition-metal impurity sites on the MgO(001) surface – a density-functional model cluster study. Chem Phys 177: 561–570

Niu C, Shepherd K, Martini D, Tong J, Kelber JA, Jennison DR, Bogicevic A (2000) Cu interactions with α-Al_2O_3 (0001): effects of surface hydroxyl groups versus dehydroxylation by Ar-ion sputtering. Surf Sci 465: 163–176

Nygren MA, Gay DH, Catlow RA (1997) Hydroxylation of the surface of the corundum basal plane. Surf Sci 380: 113–123

Payne MC, Teter MP, Allan DC, Arias TA, Joannopoulos JD (1992) Iterative minimisation techniques for ab initio total-energy calculations: molecular dynamics and conjugate gradients. Rev Mod Phys 64: 1045–1097

Puchin VE, Gale JD, Schluger AL, Kotomin EA, Günster J, Brause M, Kempter V (1997) Atomic and electronic structure of the corundum (0001) surface: comparison with surface spectroscopies. Surf Sci 370: 190–200

Schildbach MA,_Hamza AV (1993). Clean and water-covered sapphire (1 102) surfaces – structure and laser-induced desorption. Surf Sci 282: 306–322

Snyder JA, Jaffe JE, Gutowski M, Lin Z, Hess AC (2000) LDA and GGA calculations of alkali metal adsorption at the (001) surface of MgO J Chem Phys 112: 3014–3022

Sposito G (1986) In: Davis JA, Hayes KF (eds) Geochemical processes at mineral surfaces ACS Symposium Series 323, American Chemical Society, Washington, DC, pp 217–228

Stará I, Zeze D, Matolín V, Pavluch J, Gruzza B (1997) AES and EELS study of alumina model catalyst supports. Appl Surf Sci 115: 46–52

Stefanovich EV, Truong TN (1997) A theoretical approach for modeling reactivity at solid–liquid interfaces. J Chem Phys 106: 7700–7705

Stevens WJ, Basch H, Krauss J (1984) Compact effective potentials and efficient shared-exponent basis-sets for the 1st-row and 2nd-row atoms. J Chem Phys 81: 6026–6033

Stevens WJ, Krauss M, Basch H, Jasien PG (1992) Relativistic compact effective potentials and efficient, shared-exponent basis-sets for the 3rd-row, 4th-row, and 5th-row atoms. Can J Chem 70: 612–630

Stumm W (1987) Aquatic surface chemistry Wiley Interscience, New York

Sverjensky DA, Sahai N (1996) Theoretical prediction of single-site surface-protonation equilibrium constants for oxides

and silicates in water. Geochim Cosmochim Acta 60: 3773–3797

Tepesch PD, Quong AA (2000) First-principles calculations of α-alumina (0001) surfaces energies with and without hydrogen. Phys Stat Sol 217: 377–387

Vaughan DJ, Pattrick RAD (eds) (1995) Mineral surfaces. Chapman and Hall, London

Wander A, Searle B, Harrison NM (2000) An ab initio study of α-Al_2O_3 (0001): the effects of exchange and correlation functionals. Surf Sci 458: 25–33

Warren MC, Dove MT, Redfern SAT (2000) Ab initio simulations of cation ordering in oxides: application to spinel. J Phys Condens Matter 12: L43–L48

Wittbrodt JM, Hase WL, Schlegel HB (1998) Ab initio study of the interaction of water with cluster models of the aluminum terminated (0001) α-aluminum oxide Surface. J Phys Chem (B) 102: 6539–6548

Wyckoff RWG (1978) Crystal structures, Interscience Publishers, New York

Yudanov I, Pacchioni G, Neyman K, Rösch N (1997) Systematic density functional study of the adsorption of transition metal atoms on the MgO(001) surface. J Phys Chem (B) 101: 2786–2792